

**Sustainable orientation of polar molecules induced by half-cycle pulses**

A. Matos-Abiague\* and J. Berakdar†

*Max-Planck Institut für Mikrostrukturphysik, Weinberg 2, 06120 Halle, Germany*

(Received 8 September 2003; published 18 December 2003)

Subjecting polar linear molecules to appropriately designed half-cycle electromagnetic pulses induces strong orientation of the molecules. This is deduced by inspecting the quantum dynamics within a simplified model which yields analytical conditions for the parameters of the pulses that lead to strong molecular orientation sustainable for hundreds of picoseconds. These analytical predictions are largely confirmed by a full numerical time-dependent study of the orientation process for NaI molecules. Further strategies for increasing and maintaining the molecular orientation are proposed and numerically illustrated. Our finite-temperature calculations demonstrate that the molecular orientation persists at considerable temperatures.

DOI: 10.1103/PhysRevA.68.063411

PACS number(s): 32.80.Lg, 02.30.Yy, 33.80.-b

**I. INTRODUCTION**

In most cases chemical reactions are sensitive to the relative orientations of the reactants [1–3]. Therefore it is highly desirable to develop a strategy for orienting the molecules in a particular way and in a controlled manner. This is also true for laser-induced isomerization [4], molecular trapping [5], catalysis [6], high-order harmonic generation [7], and nanofabrication employing laser focusing of molecular beams [5,8].

It is well known [7,9–15] that orienting or aligning molecules can be achieved in several ways using static or time-dependent electromagnetic fields. Of particular interest for the present study is the possibility of inducing a strong orientation of a polar linear molecule by subjecting it to electromagnetic half-cycle pulses (HCPs). This is insofar interesting as by applying a HCP molecular orientation is achievable without disturbing the electronic and vibrational modes of the molecule [11,12,14]. When the pulse is turned off the molecule remains oriented [11–13]. In previous studies it has been shown that, for postpulse times, a moderate molecular orientation persists for a few picoseconds only [7,9–13].

We show in the present study that following a certain scheme specified below, a strong (compared to previous strategies) molecular orientation is achievable using HCPs. This molecular orientation can be maintained up to hundreds of picoseconds. The basic idea is to find the parameters for designing the appropriate train of ultrashort HCPs. To this end, we start by inspecting a simple analytical model that consists of a two-level system subject to a train of ultrashort HCPs. This model is too crude for describing all the facets of the quantum dynamics of the molecule. However, as shown below, it is useful insofar as the parameters of the optimal pulse sequence can be deduced analytically (for achieving maximal orientation). The analytical predictions are then employed as a rough guide for more elaborated studies of the time evolution of the molecule under the action of the designed train of HCPs. Below, we present and analyze full

numerical calculations of the time-dependent probability density as well as of the molecular orientation as obtained from an (numerically) exact solution of the time-dependent Schrödinger equation. Further numerical strategies for increasing and maintaining the molecular orientation are also proposed and demonstrated by numerical examples. These schemes include the whole spectrum and hence are beyond the capability of the two-level model. The calculations are also performed at finite temperatures, and it is demonstrated that considerable molecular orientation can be induced and maintained at temperatures as high as 10 K.

The paper is organized as follows. In Sec. II we provide the details of the theoretical model utilized for studying the time evolution of a diatomic molecule subject to a sequence of HCPs. A two-level system approximation is also developed in Sec. II, and the time dependence of the molecular orientation is studied using this analytical model. Calculational details and the results are discussed in Secs. III and IV, respectively. Finally, a brief summary is given in Sec. V.

**II. THEORY****A. Model**

In this study we are concerned with a diatomic molecule that resides in the electronic ground state. We consider those molecules that have a relatively large permanent dipole moment and a large moment of inertia, as a prototypical example we study below NaI. The molecule is subject to a train of ultrashort HCPs. The HCPs are chosen such that the duration of a single HCP is much smaller than the rotational period  $\tau_{rot}$  of the molecule (for NaI  $\tau_{rot}=138$  ps). HCPs with these characteristics are readily available nowadays. HCPs with peak fields of several hundreds of kV/cm and a duration in the subpicosecond regime are achievable [16,17]. Of particular importance for this study is the ability of designing trains of ultrashort HCPs [18–20].

Below, we employ HCPs that have a duration of the order of 0.5–1 ps. The peak amplitudes of the HCPs are up to 600 kV/cm. These parameters of the peak HCP amplitudes ensure that the molecule is not damaged upon the action of the HCPs train [11,12]. In addition, vibrational modes are not excited by such pulses [11,12]. It should be noted at this stage that, according to Maxwell's equations for a freely

\*Email address: amatos@mpi-halle.de

†Email address: jber@mpi-halle.de

propagating electromagnetic wave, the time integral over the electric field should be zero. Hence, a HCP is in fact a strongly asymmetric monocycle pulse that consists of a very short, strong half-cycle (only this part is usually referred to as a HCP), followed by a much slower half-cycle of an opposite polarity and a much smaller amplitude (called the HCP tail). Typical pulse amplitude asymmetry is 13:1. For the present molecule and for the specific parameters of the HCP used below it turned out that the tail of the HCP has hardly an influence on the results shown below.

For the properties of the molecule and the HCPs, as specified above, the quantum dynamics of the molecule subject to the HCP is correctly described by the rigid-rotor approximation [10–12]. Within this approximation the dynamics of the system is determined by the following time-dependent Schrödinger equation:

$$i\hbar \frac{\partial \Psi(\theta, \phi, t)}{\partial t} = \left[ \frac{L^2}{2I} - \mu_0 V(t) \cos(\theta) \right] \Psi(\theta, \phi, t). \quad (1)$$

We consider a diatomic molecule with a permanent dipole moment  $\mu_0$ . The reduced mass of the nuclei is denoted by  $m$ . The moment of inertia at the internuclear equilibrium distance  $R_0$  is referred to as  $I = mR_0^2$  and  $L$  is the angular-momentum operator. The polar and the azimuthal angles between the molecular axis and the applied field are denoted, respectively, by  $\theta$  and  $\phi$ . As can be seen from Eq. (1) the applied HCPs are supposed to be linearly polarized with a time-dependent envelope  $V(t)$ . In the impulsive approximation, the shape function  $V(t)$  is described satisfactorily by a series of  $N$  consecutive *kicks*, i.e.,

$$V(t) = \sum_{k=1}^N \Delta p_k \delta(t - t_k). \quad (2)$$

The time at which the  $k$ th pulse is applied is denoted by  $t_k$ . The quantity  $\Delta p_k$  is the area enclosed by the  $k$ th pulse (the time integral over the pulse), i.e., the momentum transferred to the molecule by the  $k$ th pulse.

If the applied HCPs are linearly polarized and in the absence of any other symmetry breaking fields the molecule retains the cylindrical symmetry around the molecular axis. As a consequence, the projection of the angular momentum  $M_J$  onto the field polarization axis is conserved. The time-dependent wave function that describes the quantum dynamics of the molecule under the action of the HCPs can be written as an expansion in terms of the stationary eigenstates, namely,

$$\Psi_M(\theta, \phi, t) = \sum_{J=0}^{J_{max}} C_{J,M}(t) Y_{J,M}(\theta, \phi). \quad (3)$$

We assume that the initial value of  $M_J$  is  $M$ .  $Y_{J,M}(\theta, \phi)$  are the spherical harmonics, and  $J_{max}$  is the highest eigenstate which is relevant for the time evolution of the system.

Substituting Eq. (3) into Eq. (1) we obtain the following system of differential equations for determining the expansion coefficients:

$$i\hbar \frac{\partial \mathbf{C}_M(t)}{\partial t} = \mathbf{E}_M \mathbf{C}_M(t) - \mu_0 V(t) \mathbf{U}_M \mathbf{C}_M(t), \quad (4)$$

where  $\mathbf{C}_M(t)$  is a vector of the form

$$\mathbf{C}_M(t) = (C_{0,M}(t), C_{1,M}(t), \dots, C_{J_{max},M}(t))^T. \quad (5)$$

The matrix  $\mathbf{U}_M$  is composed of the elements

$$U_{J_M, J'_M} = \langle Y_{J_M}(\theta, \phi) | \cos \theta | Y_{J'_M}(\theta, \phi) \rangle. \quad (6)$$

Furthermore, we define

$$\mathbf{E}_M = \text{diag}(E_{0,M}, E_{1,M}, \dots, E_{J_{max},M}), \quad (7)$$

where  $E_{J,M}$  are the eigenenergies of the unperturbed molecule.

Integrating Eq. (4) over the time we obtain the following stroboscopic map from  $t = t_k$  to  $t = t_{k+1}$ :

$$\mathbf{C}_M^{(k+1)} = e^{i(\mu_0 \Delta p_k / \hbar) \mathbf{U}_M} e^{-(i/\hbar) \mathbf{E}_M (t_{k+1} - t_k)} \mathbf{C}_M^{(k)}. \quad (8)$$

In this relation we introduced the notation  $\mathbf{C}_M^{(n)} = \mathbf{C}_M(t_n)$  and employed the initial condition  $\mathbf{C}_M^{(0)} = \mathbf{C}_M(t=0)$ . In addition to the stroboscopic description [Eq. (8)] of the wave-function evolution, a (continuous) propagation between consecutive pulses is performed. This can be done by noting that between consecutive kicks the system evolves field-free. Therefore, the system dynamics can be described in the time intervals  $t_k \leq t < t_{k+1}$  by

$$\mathbf{C}_M(t) = e^{-(i/\hbar) \mathbf{E}_M (t - t_k)} \mathbf{C}_M^{(k)}, \quad t_k \leq t < t_{k+1}. \quad (9)$$

Alternating Eqs. (8) and (9) the all-time evolution of the system is obtained.

The degree of the orientation of the molecule can be characterized by the expectation value

$$\langle \cos \theta \rangle_M(t) = \langle \Psi_M(\theta, \phi, t) | \cos \theta | \Psi_M(\theta, \phi, t) \rangle. \quad (10)$$

The orientation parameter  $\langle \cos \theta \rangle_M(t)$  varies in the interval  $[-1, 1]$ . Perfect orientation is signified by an extremal value of  $\langle \cos \theta \rangle_M(t)$ . A direct visual picture of the overall quantum dynamics of the system is offered by the angular-resolved, time-dependent probability density

$$P_M(\theta, t) = \int_0^{2\pi} |\Psi_M(\theta, \phi, t)|^2 d\phi. \quad (11)$$

The quantities  $\langle \cos \theta \rangle_M(t)$  and  $P_M(\theta, t)$  are the central objects of the analytical and the numerical analysis presented in the following sections.

Due to the smallness of the rotational level spacing the rotational modes can be thermally excited. Therefore, a realistic treatment has to include the effects of finite temperatures  $T$  and to include the thermal average. For the orientation parameter the thermal average  $\langle \langle \cos \theta \rangle \rangle(t)$  is obtained at low temperatures from the relation

$$\langle\langle \cos \theta \rangle\rangle(t) = Z^{-1} \sum_{J=0}^{J_{max}} P(J) \sum_{M_J=-J}^J \langle \cos \theta \rangle_{J,M_J}(t). \quad (12)$$

In the equation above  $\langle \cos \theta \rangle_{J,M_J}$  refers to the orientation parameter corresponding to a molecule initially in the  $|J, M_J\rangle$  stationary state. The function

$$P(J) = \exp\left[\frac{-BJ(J+1)}{k_B T}\right] \quad (13)$$

is the Boltzmann distribution function associated with the rotational states.  $B = \hbar^2/(2I)$  is the rotational constant of the molecule and  $k_B$  is the Boltzmann constant. The partition function is denoted by

$$Z = \sum_{J=0}^{J_{max}} (2J+1)P(J). \quad (14)$$

### B. Two-level system approximation

For a clear understanding of the time evolution of the system we develop in this section a two-level system approximation (TLSA). This approximation is based on the assumption that only the two lowest eigenstates are involved in the system evolution. The TLSA is in general of a limited validity, in particular it breaks down with increasing temperatures and/or for strong HCPs. Under appropriately chosen conditions, however, the TLSA provides a useful and comprehensive picture of the evolution of the system. In addition, as detailed below it is possible to deduce from this model analytical conditions for optimal control of the molecular orientation.

Within the TLSA the complex vector  $\mathbf{C}_M$  reduces to a two-dimensional spinor. For our purpose it is convenient to perform a transformation from the spinor space to a real space. It can be done through a transition from  $SU(2)$  to  $SO(3)$  by introducing the Bloch vector  $\mathbf{B} = (B_x, B_y, B_z)$  whose components are given by

$$B_i = \mathbf{C}_M^\dagger \sigma_i \mathbf{C}_M, \quad i = x, y, z, \quad (15)$$

where  $\sigma_i$  represent the Pauli matrices. The evolution of the system is then described by rotations of the real vector  $\mathbf{B}$  with the constraint  $|\mathbf{B}| = 1$  imposed by the normalization of the wave function.

From Eqs. (8), (9), and (15) we obtain that the action of the  $k$ th pulse on the system is determined, in the Bloch space, by the following relation:

$$\mathbf{B}(t_k) = \begin{pmatrix} 1 & 0 & 0 \\ 0 & \cos \alpha_k & -\sin \alpha_k \\ 0 & \sin \alpha_k & \cos \alpha_k \end{pmatrix} \mathbf{B}(t_k^-), \quad (16)$$

where

$$\alpha_k = \frac{2\mu_0 \Delta p_k}{\hbar \sqrt{3}}, \quad (17)$$

and  $t_k^- = t_k - \epsilon$  (with  $\epsilon \rightarrow 0^+$ ) and  $t_k$  refer to the times just before and right after the  $k$ th pulse, respectively. On the other hand the field-free evolution of the system in the time intervals  $t_k \leq t < t_{k+1}$  is determined by

$$\mathbf{B}(t) = \begin{pmatrix} \cos \beta_k & -\sin \beta_k & 0 \\ \sin \beta_k & \cos \beta_k & 0 \\ 0 & 0 & 1 \end{pmatrix} \mathbf{B}(t_k), \quad (18)$$

where

$$\beta_k = \frac{2\pi(t-t_k)}{\tau_{rot}} \quad (19)$$

and  $\tau_{rot}$  denotes the rotational period of the molecule. Equations (16) and (18) offer a clear geometrical interpretation of the evolution of the system. The action of the  $k$ th pulse represents a counterclockwise rotation of the Bloch vector  $\mathbf{B}$  by an angle  $\alpha_k$  round the  $x$  axis, while the field-free motion between the  $k$ th and the  $(k+1)$ th pulses amounts to rotating  $\mathbf{B}$  counterclockwise by an angle  $\beta_k$  round the  $z$  axis.

Within the TLSA the orientation parameter [Eq. (10)] can be rewritten in terms of the Bloch vector as follows:

$$\langle \cos \theta \rangle_M(t) = \frac{1}{\sqrt{3}} B_x(t). \quad (20)$$

In the Bloch space, the initial state of the system is given by the vector  $(0,0,1)$  (note that this vector is invariant to rotations round the  $z$  axis, i.e., it actually represents a stationary state), while the state of optimal orientation corresponds to the vector  $(1,0,0)$  [see Eq. (20)]. The process of inducing molecular orientation consists then in transforming the vector  $(0,0,1)$  into  $(1,0,0)$  through rotations around the  $x$  and  $z$  axes. One then searches for pulse parameters of field-induced rotations that leave quasi-invariant the Bloch vector  $(1,0,0)$  corresponding to the optimal molecular orientation. This simple geometrical interpretation leads to the procedure illustrated in Fig. 1 for inducing and maintaining the molecular orientation of a molecule initially in its rotational ground state. One applies, at  $t = t_1^- = -\epsilon$  ( $\epsilon \rightarrow 0^+$ ), an auxiliary pulse with a peak amplitude such that  $\alpha_1 = \pi/2$  and the initial Bloch vector  $(0,0,1)$  evolves to  $(0, -1, 0)$  [see Fig. 1(a)]. After a subsequent time delay, at  $t = t_2^- = (\tau_{rot}/4) + \gamma - \epsilon$  ( $\gamma \ll \tau_{rot}/4$ ,  $\epsilon \rightarrow 0^+$ ), the Bloch vector evolves as shown in Fig. 1(b) and the molecule is well oriented [note that now the vector  $\mathbf{B}$  is close to the vector  $(1,0,0)$  corresponding to the optimal molecular orientation]. Figure 1(c) shows the Bloch vector at  $t = t_2$ , after the application of a second pulse at  $t = t_2^-$  with pulse parameters such that  $\alpha_2 = \pi$ . Then, upon a time delay  $2\gamma$ , the Bloch vector evolves again to the position depicted in Fig. 1(b). Iterating this procedure the Bloch vector oscillates between the positions displayed in Figs. 1(b) and 1(c), i.e., in a close vicinity of the vector  $(1,0,0)$ . Thus, following this scheme the molecule attains and maintains nearly its maximal orientation  $\langle \cos \theta \rangle \approx 1/\sqrt{3}$  [see Eq. (20)] until the train of pulses is turned off.

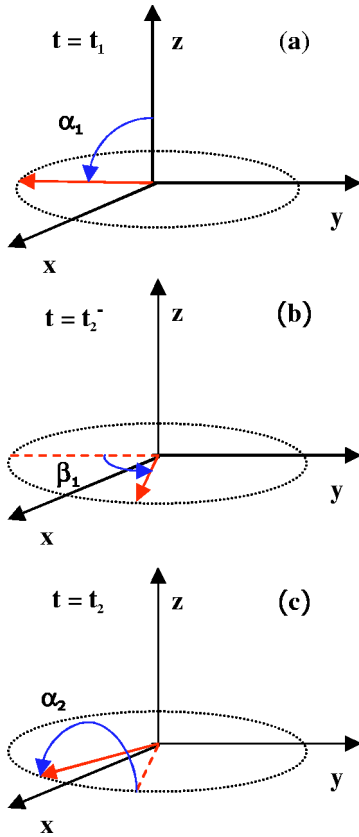


FIG. 1. (Color online) Geometrical illustration of the time evolution of the system. (a) The Bloch vector at  $t=t_1=0$ . (b) The Bloch vector at  $t=t_2^-(\tau_{rot}/4)+\gamma-\epsilon$  ( $\gamma \ll \tau_{rot}/4$ ,  $\epsilon \rightarrow 0^+$ ). (c) The position of the Bloch vector at the time  $t=t_2$ .

Summarizing, the TLSA leads to the following sequence of HCPs for a large sustainable molecular orientation: One applies, at first, an auxiliary pulse with a peak amplitude that provides the kick  $\Delta p_1 = \sqrt{3}\hbar\pi/(4\mu_0)$  (i.e.,  $\alpha_1 = \pi/2$ ) and, after a time delay  $t_2 - t_1 = (\tau_{rot}/4) + \gamma$ , a periodic train of HCPs with period  $\tau_p \approx 2\gamma$  and  $\Delta p_k = 2\Delta p_1$  ( $k > 1$ ). The value of  $\gamma$  can be arbitrarily chosen within the restriction  $\gamma \ll \tau_{rot}/4$  but not too small (to avoid the overlap of consecutive pulses).

The geometrical interpretation discussed above offers the following physical picture of the evolution of the system which serves as the basis for the control schemes proposed here (it will be shown below that this picture is not only valid for TLSA but also viable for the general case). The application of an auxiliary HCP (or several auxiliary pulses as discussed in the following section) creates a rotational wave packet. Applying the external field the molecule begins to orientate along the field direction until it reaches a maximum orientation. We recall that the molecules considered here have a large moment of inertia. Therefore, once the maximum molecular orientation is achieved, the molecule reverses its rotational motion to orientation in the opposite direction. This process of reaching maximal orientation followed by orientation reversal is periodically repeated. This is because after the pulse has passed by, the molecule evolves in a field-free fashion. Strong molecular orientation is only

achieved at time intervals close to the time at which the molecule reaches its optimal orientation. As a result of this behavior, if we subject the molecule only to a single pulse we cannot achieve a sustainable molecular orientation. In fact, within a rotational period, the time average of the orientation parameter vanishes [11,12].

The above picture of the creation and the time evolution of the molecular orientation changes if a second HCP is applied at the time when the molecule reaches the maximal orientation (due to the first HCP) and starts to reverse its rotational motion [cf. Fig. 1(b)]. Provided the second pulse is strong enough, a new reversal of the rotational wave packet motion is induced. Consequently, the molecule returns to its maximal orientation [cf. Fig. 1(c)].

From the above we conclude that the application of several appropriately designed pulses renders possible the creation of sustainable molecular orientation lasting as long as the duration of the train of HCPs. The ideas behind this scheme are also valid in the general case when all the levels participate in the evolution of the system. The key question for practical implementation of the scheme is how to determine the parameters of the required pulses. The first hint for answering this question was provided by our discussion of the TLSA. However, as the TLSA is not valid for arbitrary values of the pulse parameters and is expected to fail especially when increasing temperatures, we also performed full numerical calculations for the optimization of the molecular orientation. These calculations are discussed in the following sections.

### III. CALCULATION DETAILS

In the general case, when subjecting the molecule to a strong HCP at finite  $T$ , a large number of levels has to be included for a proper treatment of the time evolution of the system. An analytical approach becomes then intractable and one has to resort to full numerical methods. This section provides the details of the numerical model for optimizing the molecular orientation.

To obtain the wave function [Eq. (3)] one has to determine the expansion coefficients. Those are deduced from Eq. (9) between consecutive pulses and from the matching conditions, Eq. (8), at the time steps when the pulses are applied. The quantities characterizing the molecular orientation are then evaluated using Eqs. (10) and (11). The highest relevant angular-momentum value  $J_{max}$  of  $J$  is determined by inspecting the convergence condition

$$\sum_{J=0}^{J_{max}} \sum_{M_J=-J}^J |C_{J,M}|^2 \approx 1, \quad (21)$$

which states that the angular-momentum states beyond  $J_{max}$  are irrelevant.

In this work we study NaI molecules. This particular molecule is chosen as prototypical example for a polar molecule with a large moment of inertia (the rotational constant  $B \approx 0.12 \text{ cm}^{-1}$ ) and has a permanent dipole  $\mu_0 = 9.2D$ . As stated in the Introduction, for the treatment of the HCPs within the impulsive approximation, it is essential for the

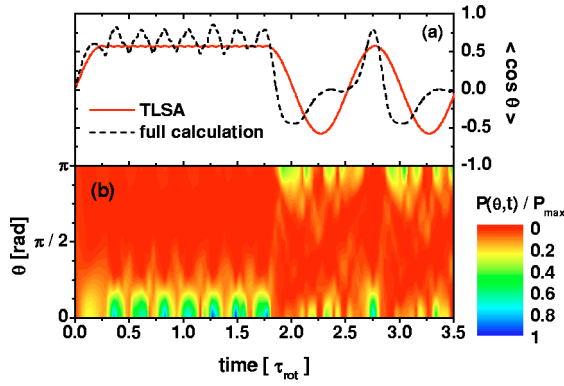


FIG. 2. (Color online) (a) The time dependence of the orientation parameter  $\langle \cos \theta \rangle$  in units of the rotational period of the molecule. The pulse width is 1 ps ( $\approx 0.0072\tau_{rot}$ ). The optimal orientation pulse parameters are derived from the TLSA [ $t_1=0$ ,  $t_2=39.5$  ps ( $\approx 0.29\tau_{rot}$ ),  $t_k=t_2+(k-2)\tau_p$ ,  $\tau_p=10$  ps ( $\approx 0.072\tau_{rot}$ ),  $F_1=93.5$  kV/cm, and  $F_k=187$  kV/cm ( $k\geq 2$ )]. The results of the TLSA (solid curve) are shown along with the full numerical calculations (dashed curve). (b) Numerical results (including all the spectrum) for the angular and time dependence of the probability density  $P(\theta, t)$  normalized to its maximum value  $P_{max}$ . The pulse parameters are the same as in (a).

rotational period  $\tau_{rot}$  to be much larger than the pulse durations ( $\sim 0.5$ – $1$  ps). This condition is well fulfilled for NaI since its rotational period is  $\tau_{rot}=138$  ps. Thus the sudden approximation [Eq. (2)] is justified and used throughout the calculations. As done in Ref. [12], we assume sine-square HCPs with peak amplitudes  $F_k$  up to 600 kV/cm and durations in the range of  $d\sim 0.5$ – $1$  ps. The pulse areas are then obtained as  $\Delta p_k=F_k d/2$ . A reasonable choice for the ratio  $\mathcal{R}$  of the pulse duration as compared to the time delay between them is essential. This choice has to be made in such a way as to avoid the overlap of consecutive pulses. In the present study we employ for this ratio a maximum of  $\mathcal{R}=1/8$ .

The calculations were performed for the scheme provided by the TLSA in the preceding section, and further schemes based on applying multiple auxiliary pulses and a subsequent train of HCPs for optimizing the molecular orientation were also numerically implemented, as discussed in the following section.

#### IV. RESULTS

In order to test the predictions of Sec. II B, we performed a full-fledged numerical calculation with the pulse parameters predicted by the TLSA. The results are shown in Fig. 2(a), where the time dependence of the orientation parameter is displayed. As clear from Fig. 2(a), the TLSA (solid line) cannot reproduce quantitatively the full dynamics of the system (dashed line), but it is in qualitative agreement with the numerical calculation, showing that the scheme suggested in Sec. II B for inducing an efficient and sustainable molecular orientation is essentially valid even when all the levels are incorporated in the system evolution. A further useful quantity for the understanding of the time evolution of the system is the angular and time-resolved probability density  $P(\theta, t)$

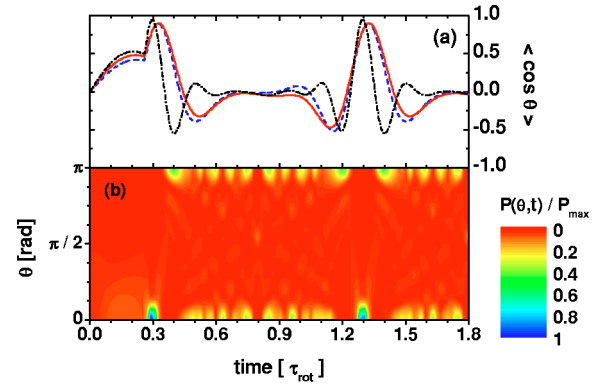


FIG. 3. (Color online) (a) Time dependence of the orientation parameter  $\langle \cos \theta \rangle$  obtained with a first pulse applied at  $t_1=0$  and a second one at  $t_2=36$  ps ( $\approx 0.26\tau_{rot}$ ) for different values of their strengths. Dashed line corresponds to  $F_1=50$  kV/cm and  $F_2=240$  kV/cm. Solid and dash-dotted lines correspond to  $F_1=60$  kV/cm and  $F_2=220$  kV/cm, and  $F_1=70$  kV/cm and  $F_2=420$  kV/cm, respectively. (b) Normalized angular distribution of the probability density corresponding to the dash-dotted line in (a) as a function of time and  $\theta$ .

which is shown in Fig. 2(b). Initially [before applying the first pulse ( $t<0$ )], the probability density  $P(\theta, t)$  is isotropically distributed, signifying the absence of orientation. After the application of the second pulse the angular distribution of  $P(\theta, t)$  is squeezed in a localized region around  $\theta=0$  [cf. Fig. 2(b)]. The strong localization (orientation) effect is time dependent and lasts for  $\tau_f\approx 250$  ps (i.e.,  $\tau_f\approx 1.8\tau_{rot}$ ). When the HCPs train is over the system evolves in a field-free manner with the rotational period of the molecule, regaining again its strong orientation at  $t\approx \tau_f+\tau_{rot}$ .

The TLSA guided us to the procedure of Fig. 2 which, compared to previous schemes (e.g., Refs. [9–13]), yields a strong and sustainable molecular orientation. On the other hand, the full numerical results indicate the possibility of achieving even stronger orientation when higher levels are included (see Fig. 2). Therefore, we envisage a second scheme based on applying two auxiliary pulses. Within this scheme we apply at first two auxiliary pulses for inducing strong orientation. The duration of the pulses is set to 1 ps ( $\approx 0.0072\tau_{rot}$ ) and the time delay between them to 36 ps ( $\approx 0.26\tau_{rot}$ ). Note that the time delay assumed is a few picosecond smaller than the value provided by the TLSA (39.5 ps) in order to take into account that when higher levels are included the orientation after the first pulse occurs faster than within the TLSA [see Fig. 2(a)]. The strengths  $F_1$  and  $F_2$  of the pulses are then numerically determined by imposing the condition  $\langle \cos \theta \rangle > 0.8$ . Several combinations obey this requirement, here we just show some of them in Fig. 3.

The results displayed in Fig. 3 are in agreement with those reported in Ref. [15], where an accumulative squeezing approach for inducing strong orientation is proposed. The scheme of Ref. [15] is based on the application of a sequence of pulses. Each pulse is then applied when the molecule, after application of the previous pulse, reaches its maximum orientation (a similar behavior can be appreciated in Fig. 3). We note, however, that the accumulative squeezing approach

proposed in Ref. [15] requires the time delay between consecutive pulses to decrease exponentially with the number of pulses, making the scheme too restrictive when a large number of pulses need to be considered (in an actual experimental situation the procedure will lead to the overlapping of the pulses). The authors of Ref. [15] proposed then to overcome this problem by the introduction of the  $\tau_{rot}$  shift (during which the time average of the orientation is zero) between the pulses. Consequently, within the accumulative squeezing approach the molecular orientation is not sustainable (in the sense that between the successive times at which the molecule is well oriented, the time average of the orientation is zero). As suggested by the TLSA, to maintain the molecular orientation induced by the auxiliary pulses for times of the order of  $\tau_{rot}$  or larger, the pulses have to be applied after the molecule has reversed its rotational motion, i.e., at certain delay time after the molecule reaches its optimal orientation.

Once the parameters of the two auxiliary pulses that lead to a strong orientation have been determined, a periodic train of HCPs which maintains the strong molecular orientation is applied. The optimal peak field and the period of the pulses are found by fixing the values of the pulse width (we assumed 1 ps) and setting the time  $t_3$  of application of the train of HCPs close to the time at which the molecule, after application of the second auxiliary pulse, has reversed its rotational motion (i.e., a short time after the molecule reaches its maximum orientation). We then compute the time average of the orientation

$$Q = \frac{1}{(\tau_f - \tau_i)} \int_{\tau_i}^{\tau_f} \langle \cos \theta \rangle(t') dt', \quad (22)$$

where  $\tau_i$  and  $\tau_f$  are the times at which the HCPs train is, respectively, applied and turned off, and determine the values of the peak field and the period of the sequence of HCPs that lead to optimal orientation, i.e., those that maximize the averaged orientation  $Q$ .

The dynamics of the molecular orientation and the angular distribution corresponding to the maximum value of  $Q$  [see Eq. (22)] are displayed in Figs. 4(a) and 4(b), respectively. The same qualitative behavior as in Fig. 2 is observed, but now the molecular orientation is stronger.

Generally, the orientation strength is destroyed at high temperatures  $T$  [10,11,13]. Thus, to achieve appreciable orientation at finite  $T$  we developed a three-auxiliary-pulses scheme. We use pulses with a duration of 0.5 ps ( $\approx 0.0036\tau_{rot}$ ) separated by a delay time of 4 ps ( $\approx 0.03\tau_{rot}$ ). The strengths of the first and the second auxiliary pulses are taken as  $F_1 = 400$  kV/cm and  $F_2 = 200$  kV/cm. Following a similar procedure as for the two-auxiliary-pulse scheme, the optimization was performed with respect to the strength  $F_3$  of the third auxiliary pulse, while keeping the peaks of the subsequent train at  $F_k = 600$  kV/cm ( $k > 3$ ). To suppress the adverse effect of the thermal average on the molecular orientation, generally stronger pulses with shorter delay times are required. That is why we have taken the limit values (within the range of pulse parameters considered here) for the duration of the

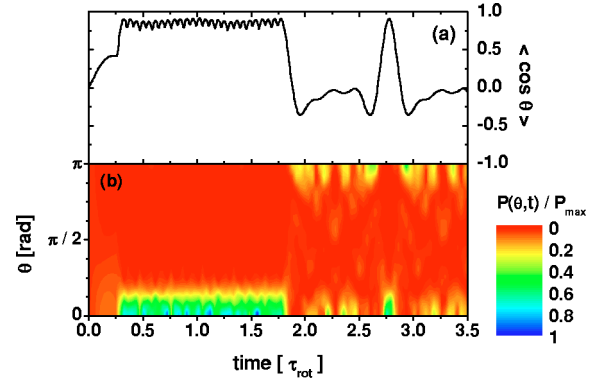


FIG. 4. (Color online) (a) Time dependence of the orientation parameter  $\langle \cos \theta \rangle$  obtained with the field parameters  $t_1 = 0$ ,  $t_2 = 36$  ps ( $\approx 0.26\tau_{rot}$ ),  $t_3 = 49$  ps ( $\approx 0.36\tau_{rot}$ ),  $t_k = t_3 + (k-3)\tau_p$ ,  $\tau_p = 8$  ps ( $\approx 0.06\tau_{rot}$ ),  $F_1 = 50$  kV/cm,  $F_2 = 240$  kV/cm, and  $F_k = 540$  kV/cm ( $k \geq 3$ ). (b) The corresponding normalized angular distribution of the probability density as a function of time and  $\theta$ .

pulses and the time delay between them as well as for the peak amplitudes of the train of HCPs.

The results are depicted in Fig. 5 when the time dependence of the thermally averaged orientation is displayed for different values of the temperature. As shown in Fig. 5, within our scheme, a strong molecular orientation (compared to other methods [10,11,13]) can be achieved and maintained even at finite temperatures. It is worth noting that the fact that the orientation shown in Fig. 5 is maintained for a shorter interval of time than in the case of Fig. 4 is not a temperature effect. It is due to the fact that in Fig. 5 the period of the pulses has been set to a half of the period used in Fig. 4 while keeping the same number of applied kicks. Therefore one can maintain the molecular orientation for larger times by applying more pulses.

## V. CONCLUSION

The prime motivation of this work is to identify the parameters of HCPs that, when applied to a polar linear molecule, lead to strong molecular orientation. To achieve this

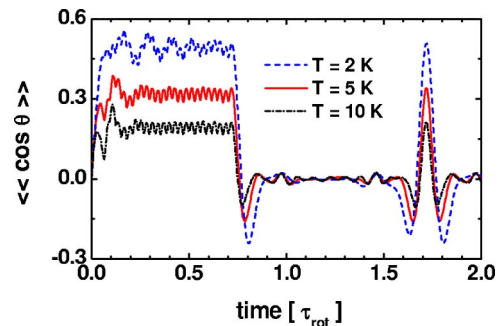


FIG. 5. (Color online) The thermal average ( $\langle \langle \cos \theta \rangle \rangle$ ) of the orientation parameter vs the time at different temperatures  $T$  as depicted in the figure. HCPs are applied at times  $t_l = (l-1)\tau_p$  [ $\tau_p = 4$  ps ( $\approx 0.03\tau_{rot}$ ),  $l \geq 1$ ] with strengths  $F_1 = 400$  kV/cm,  $F_2 = 200$  kV/cm,  $F_k = 600$  kV/cm ( $k > 3$ ). The optimal values of  $F_3$  are found to be about 375 kV/cm, 528 kV/cm, and 593.6 kV/cm for temperatures 2 K, 5 K, and 10 K, respectively.

goal we started from a simplified two-level approximation that yields analytical results for the appropriate pulse parameters. The prediction of this model serves as a starting point for full numerical calculations including the complete spectrum of the system. Based on numerical optimization, we

suggest further a procedure for inducing and sustaining a strong molecular orientation. Finite-temperature effects are included in the calculations, and it is shown that the molecular orientation achieved within our method is robust to thermal averaging.

- 
- [1] P.R. Brooks, *Science* **193**, 11 (1976).  
[2] H.J. Loesch and A. Remscheid, *J. Chem. Phys.* **93**, 4779 (1990).  
[3] F.J. Aoiz *et al.*, *Chem. Phys. Lett.* **289**, 132 (1998).  
[4] C.M. Dion *et al.*, *J. Chem. Phys.* **105**, 9083 (1996).  
[5] T. Seideman, *Phys. Rev. A* **56**, R17 (1997).  
[6] M.G. Tenner, E.W. Kuipers, A.W. Kleyn, and S. Stolte, *J. Chem. Phys.* **94**, 5197 (1991).  
[7] H. Stapelfeldt and T. Seideman, *Rev. Mod. Phys.* **75**, 543 (2003).  
[8] H. Stapelfeldt, H. Sakai, E. Constant, and P.B. Corkum, *Phys. Rev. Lett.* **79**, 2787 (1997).  
[9] M.J.J. Vrakking and S. Stolte, *Chem. Phys. Lett.* **271**, 209 (1997).  
[10] L. Cai, J. Marango, and B. Friedrich, *Phys. Rev. Lett.* **86**, 775 (2001).  
[11] M. Machholm and N.E. Henriksen, *Phys. Rev. Lett.* **87**, 193001 (2001).  
[12] C.M. Dion, A. Keller, and O. Atabek, *Eur. Phys. J. D* **14**, 249 (2001).  
[13] A. Ben Haj-Yedder *et al.*, *Phys. Rev. A* **66**, 063401 (2002).  
[14] M. Leibscher, I.Sh. Averbukh, and H. Rabitz *Phys. Rev. Lett.* **90**, 213001 (2003).  
[15] I.Sh. Averbukh and R. Arvieu, *Phys. Rev. Lett.* **87**, 163601 (2001).  
[16] R.R. Jones, D. You, and P.H. Bucksbaum, *Phys. Rev. Lett.* **70**, 1236 (1993).  
[17] D. You, R.R. Jones, P.H. Bucksbaum, and D.R. Dykaar, *Opt. Lett.* **18**, 290 (1993).  
[18] A. Wetzels, A. Gürtel, H.G. Muller, and L.D. Noordam, *Eur. Phys. J. D* **14**, 157 (2001).  
[19] M.T. Frey *et al.*, *Phys. Rev. A* **59**, 1434 (1999).  
[20] B.E. Tannian *et al.*, *Phys. Rev. A* **62**, 043402 (2000); C.O. Reinhold *et al.*, *J. Phys. B* **34**, L551 (2001).